ep SCATTERING AT COLLIDERS

J. BLÜMLEIN

THEORY INTERESTS: (1990ies)

- EARLIER: INVESTIGATIONS OF DIFFERENT TREE LEVEL PROCESSES (→ NOT MUCH LEFT OVER!)

WE CONCENTRATE ON:

- ep in 1^{ST} + HO CORR.
  - QED → RC's
  - QCD → · SCALING VIOLATIONS
    · α_s MEASUREMENT, Λ
    · BEHAVIOUR OF STRFCT.
    · SMALL x PHYSICS
    • SUSY EFFECTS (J. BOTTS)
- (MORE ELABORATE) TREE LEVEL X-SECT. & THEIR RC's.
  - ep → HIGES + $O(\alpha_s) + O(\alpha)$
  - LQ's (exp. Vectors) + $O(\alpha_s) + O(\alpha)$
  - 'HEAVY SYSTEMS' ↔ DIS & PHOTOPROD.

→ OTHER CHANN e^+e^-, $p\bar{p}$ ...

WORK PARTLY DONE IN COLLABORATION WITH :

BARDIN, BARTELS, BOOS, BOTTS, FRAMPTON, GODFREY, HAUTMANN, HOLLIK, INGELMAN, KLEIN, LEIKE, LEVMAN, VAN NEERVEN, MELNIKOV, VAN OLDENBORGH, OLNESS, RÜCKL, SCHULER, SPIESBERGER,

RIEMANN + DUBNA - ZEUTHEN GROUP.

⇒ SKETCH A FEW RESEARCH DIRECTIONS

- QED CORRECTIONS : A WAY TO COMPLETENESS (→ ARBUSOV)
- SMALL x : 'OPE MOTIVATED WAY'
- INTERESTING EXCLUSIVE PROCESSES

  → $ep \to$ HIGGS + $O(\alpha_s \& \alpha)$

  LQ → BOOS

2. The Corrections up to $\mathcal{O}(\alpha^2)$

(METHOD FROM QCD) MORE GEN.: RGE.

Contributions:

1. Bremsstrahlung: Diagrams a,b
2. Electron Pair Production: Diagram c
3. Fermion Pair Production: Diagram d , $f = e, \mu, \tau, u, d, s, c, b$

The Radiator-Method is applied.

Meaning of the bullet: Collinear Bremsstrahlung contribution **including** soft & virtual corrections.

An individual consideration of initial and final state bremsstrahlung is possible.

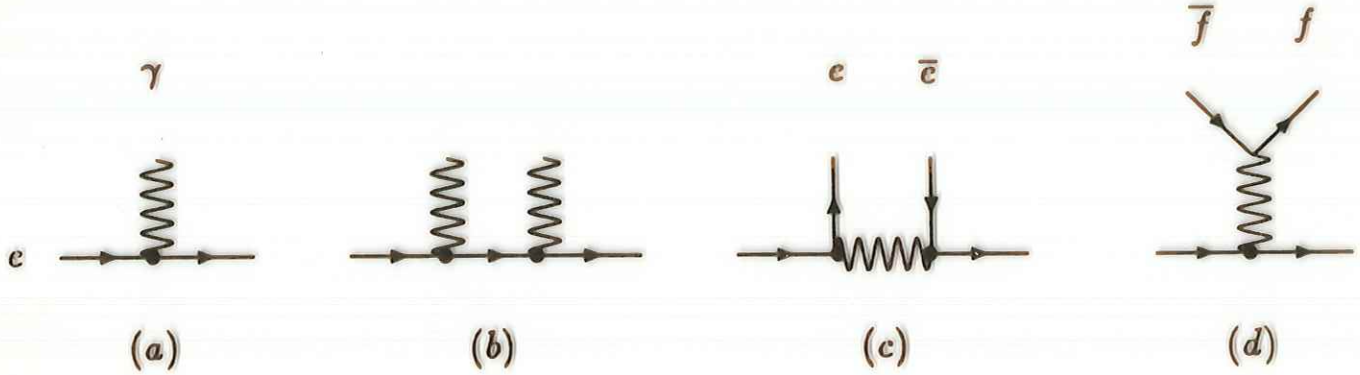

$$\frac{d^2\sigma^{(2)}}{dxdy} = \frac{d^2\sigma^{(0)}}{dxdy} + \frac{\alpha}{2\pi}\ln\left(\frac{Q^2}{m_e^2}\right)\int_0^1 P_{ee}^{(1)}(z)\left\{\theta(z-z_0)\mathcal{J}(x,y,z)\frac{d^2\sigma^{(0)}}{dxdy}|_{x=\hat{x},y=\hat{y},s=\hat{s}} - \frac{d^2\sigma^{(0)}}{dxdy}\right\}$$
$$+ \frac{1}{2}\left[\frac{\alpha}{2\pi}\ln\left(\frac{Q^2}{m_e^2}\right)\right]^2\int_0^1 P_{ee}^{(2,1)}(z)\left\{\theta(z-z_0)\mathcal{J}(x,y,z)\frac{d^2\sigma^{(0)}}{dxdy}|_{x=\hat{x},y=\hat{y},s=\hat{s}} - \frac{d^2\sigma^{(0)}}{dxdy}\right\}$$
$$+ \left(\frac{\alpha}{2\pi}\right)^2\int_{z_0}^1\left\{\ln^2\left(\frac{Q^2}{m_e^2}\right)P_{ee}^{(2,2)}(z) + \sum_{f=l,q}\ln^2\left(\frac{Q^2}{m_f^2}\right)P_{ee,f}^{(2,3)}(z)\right\}\mathcal{J}(x,y,z)\frac{d^2\sigma^{(0)}}{dxdy}|_{x=\hat{x},y=\hat{y},s=\hat{s}}$$

$$\mathcal{J}(x,y,z) = \left|\begin{array}{cc}\partial\hat{x}/\partial x & \partial\hat{y}/\partial x \\ \partial\hat{x}/\partial y & \partial\hat{y}/\partial y\end{array}\right| \tag{2}$$

$\mathcal{O}(\alpha)$

$$P_{ee}^{(1)}(z) = \frac{1+z^2}{1-z} \tag{4}$$

$$P_{ee}^{(2,1)}(z) = \frac{1}{2}\left[P_{ee}^{(1)}\otimes P_{ee}^{(1)}\right](z)$$

$\mathcal{O}(\alpha^2)$: Bremsstrahlung

$$= \frac{1+z^2}{1-z}\left[2\ln(1-z) - \ln z + \frac{3}{2}\right] + \frac{1}{2}(1+z)\ln z - (1-z) \tag{5}$$

$$P_{ee}^{(2,2)}(z) = \frac{1}{2}\left[P_{e\gamma}^{(1)}\otimes P_{\gamma e}^{(1)}\right](z)$$

: e^+e^-

$$\equiv (1+z)\ln z + \frac{1}{2}(1-z) + \frac{2}{3}\frac{1}{z}(1-z^3) \tag{6}$$

: $f\bar{f}$

$$P_{ee,f}^{(2,3)}(z) = N_c(f)e_f^2\frac{1}{3}P_{ee}^{(1)}(z)\theta\left(1-z-\frac{2m_f}{E_e}\right) \tag{7}$$

→ DESCRIBE $F_i(x,Q^2)$ FOR $Q^2 \to 0$:

$$\times\left[1-\exp(-A^2\hat{Q}^2)\right] \quad \text{with} \quad A^2 = 3.37\,\text{GeV}^{-2}. \tag{12}$$

$O(\alpha)$:

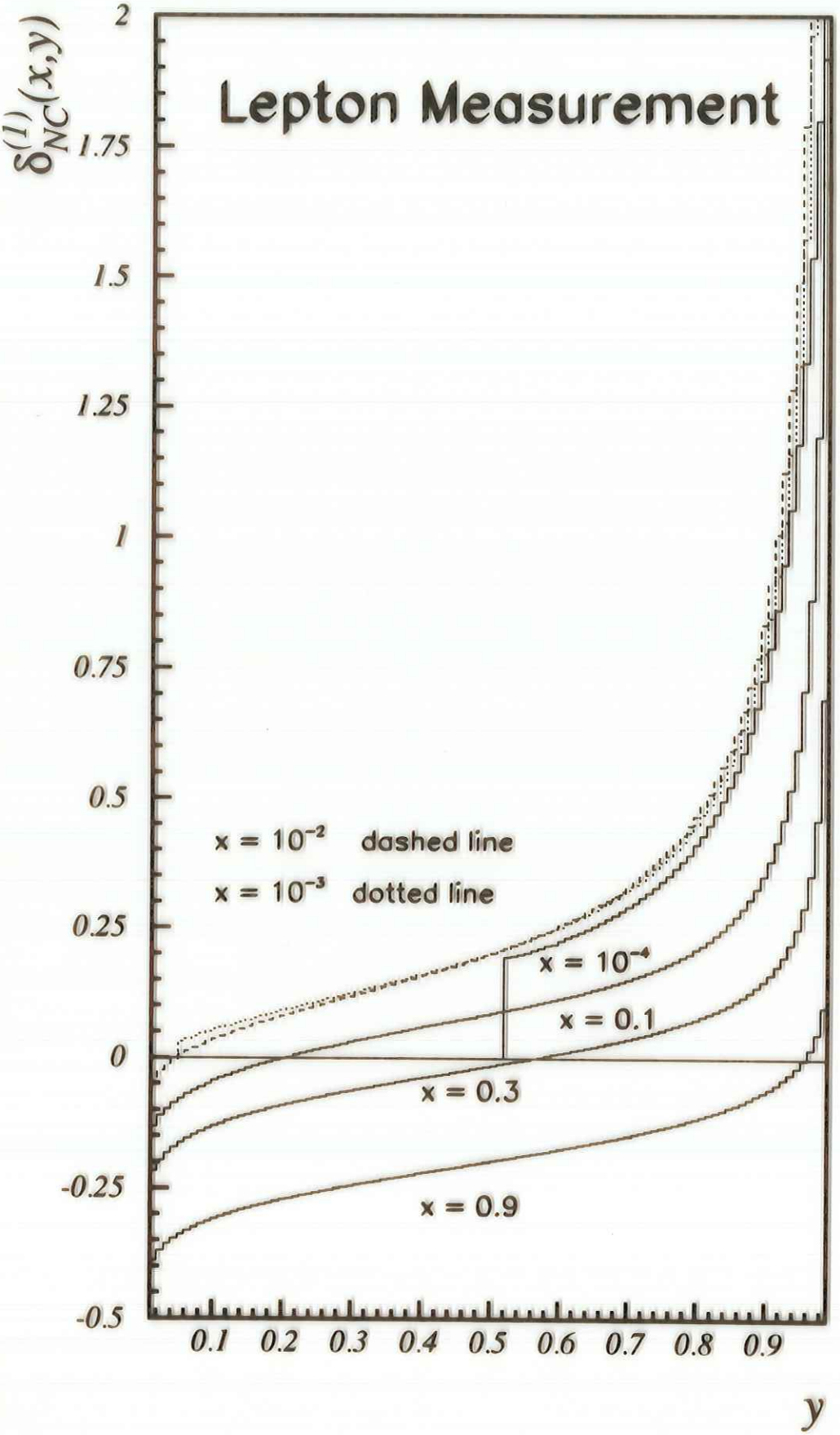
Lepton Measurement
$\delta^{(1)}_{NC}(x,y)$
2
1.75
1.5
1.25
1
0.75
0.5
0.25
0
-0.25
-0.5
0.1
0.2
0.3
0.4
0.5
0.6
0.7
0.8
0.9
y
x = 10^{-2} dashed line
x = 10^{-3} dotted line
x = 10^{-4}
x = 0.1
x = 0.3
x = 0.9

$O(\alpha^2)$

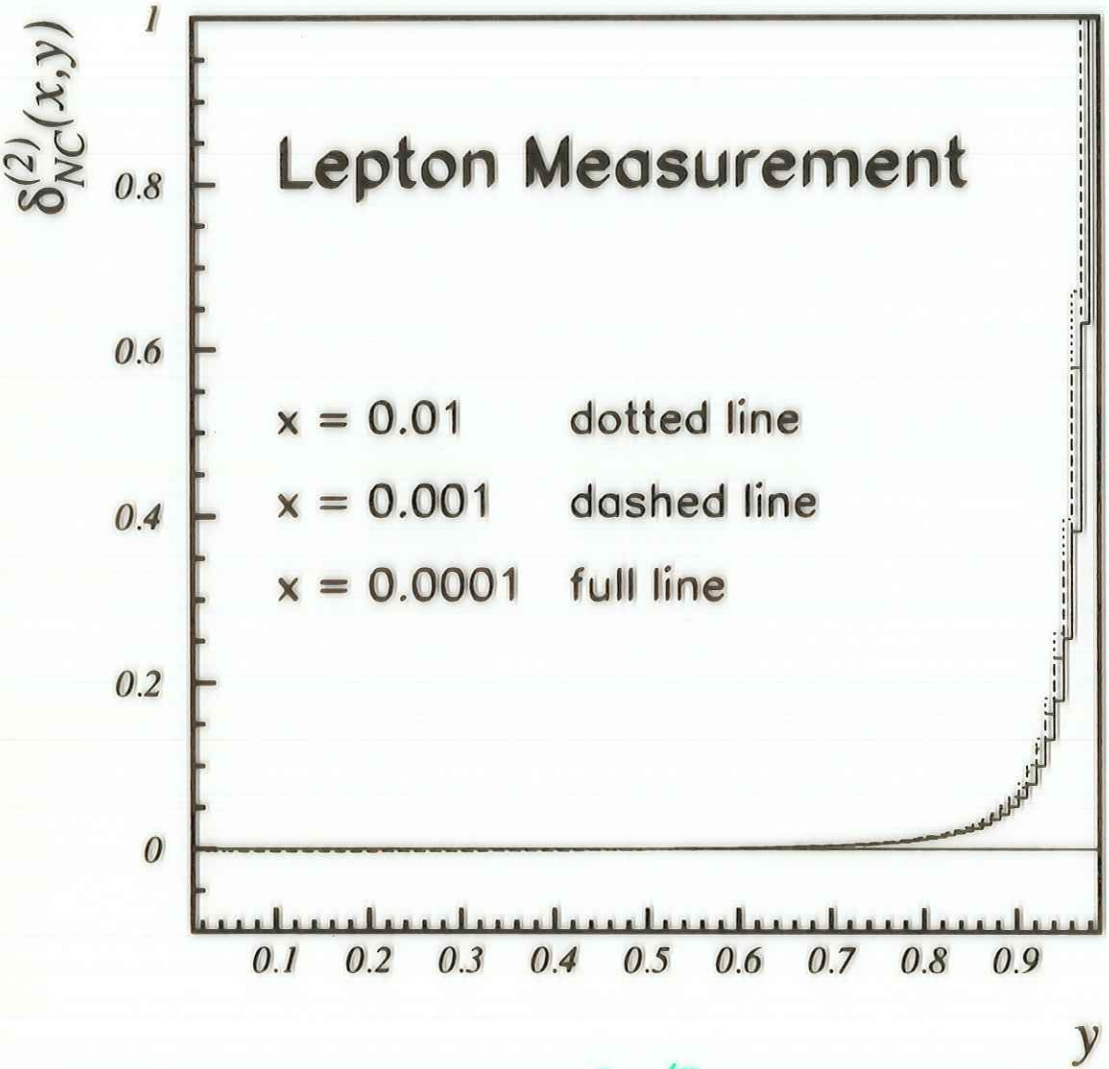

$$\delta_i^{(2)}(x,y) = \frac{\frac{d^2\sigma^{(2)}}{dx\,dy}}{\frac{d^2\sigma^{(0)}}{dx\,dy}}$$

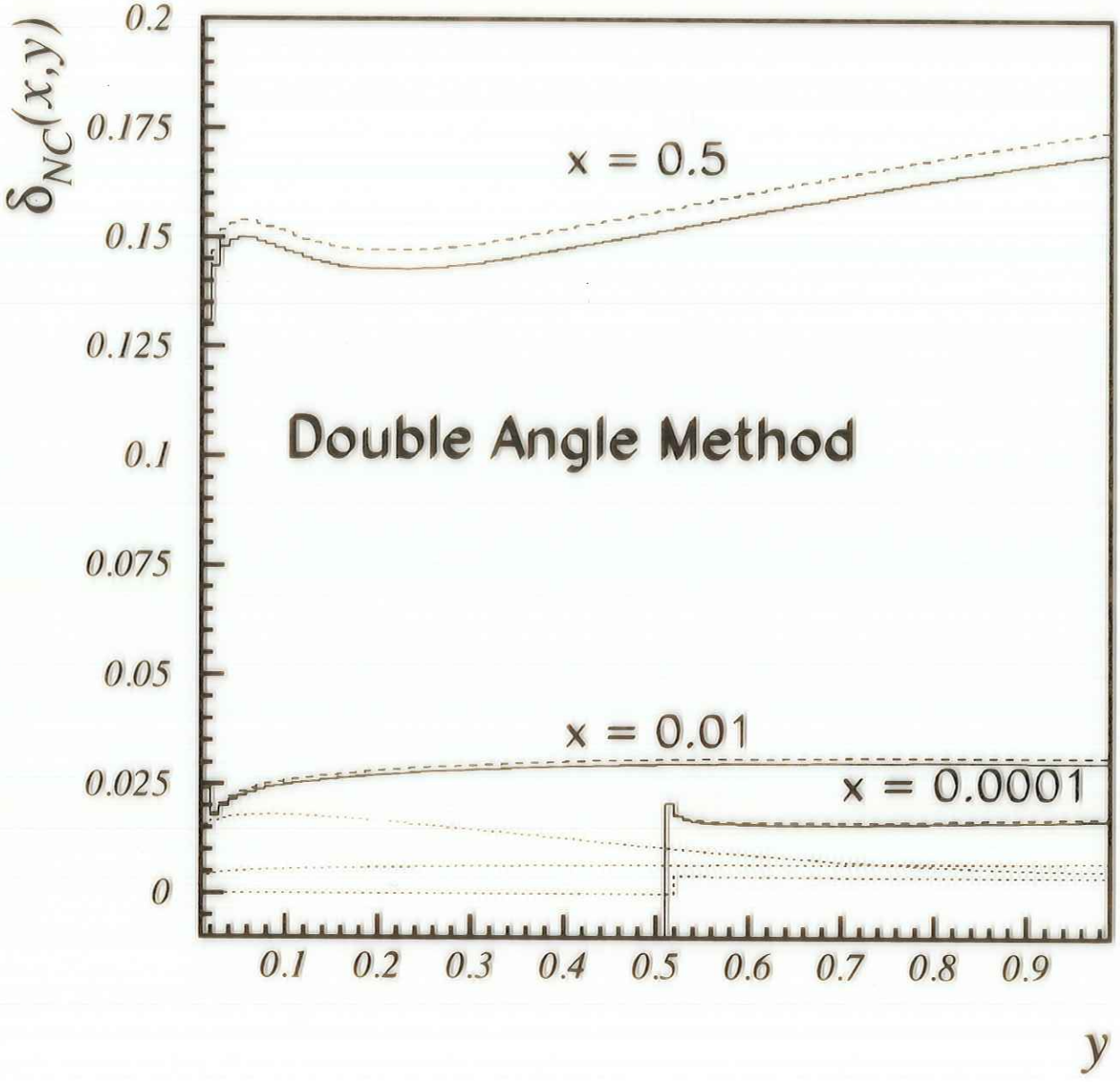

Figure 6: $\delta_{NC}(x,y)$ for the case of the double angle method for $\mathcal{A} = 35\,\mathrm{GeV}$. Full lines: $\delta_{NC}^{(1+2+>2,soft)}(x,y)$, dashed lines: $\delta_{NC}^{(1)}(x,y)$. Dotted lines: $\delta_{NC}^{e^-\to e^+}(x,y)$ scaled by $\times 100$; upper line: $x = 0.5$, middle line: $x = 0.01$, lower line: $x = 0.0001$. The other parameters are the same as in figure 3.

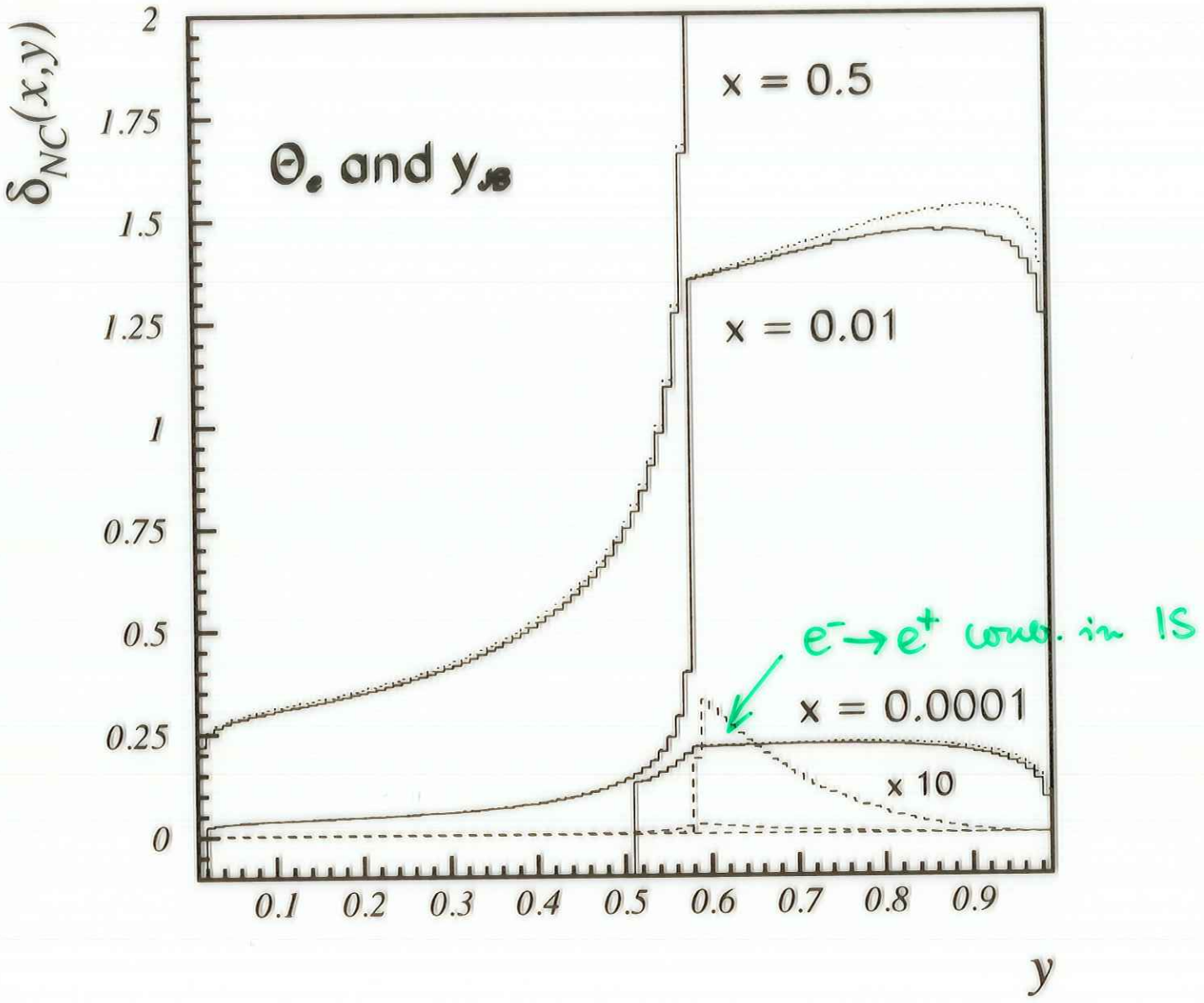

Figure 7: $\delta_{NC}(x,y)$ for the measurement based on θ_e and y_{JB} for $\mathcal{A} = 35\,\mathrm{GeV}$. Full lines: $\delta_{NC}^{(1+2+>2,soft)}(x,y)$, dotted lines: $\delta_{NC}^{(1)}(x,y)$. Dashed lines: $\delta_{NC}^{e^-\to e^+}(x,y)$; upper line: $x = 0.5$, middle line: $x = 10^{-2}$, lower line: $x = 10^{-4}$. The other parameters are the same as in figure 3.

SMALL x EFFECTS IN STRUCTUREFUNCTIONS

... DEPARTURE FROM AP eqs.

⟶ SCREENING, RESTORE UNITARITY

GLR

- FIRSTLY QUANTIFIED

⟶ $k_\perp$ FACTORIZATION

BFKL & SF's IN A CONSEQU. WAY.

NNLO : ⟶ NUM., RESUMMATION (⟶ J. BOTTS)

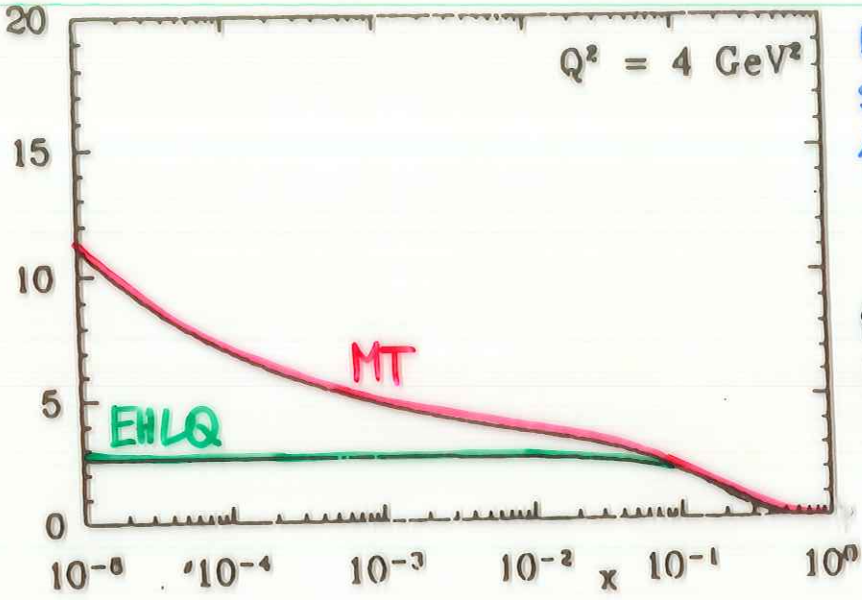

a

BARTELS, JB, SCHULER 1990

(cf. COLLINS, KWIECINSKI 1990; ALTMANN, GLÜCK, REYA, 1992 FOR SIMILAR INVESTIG.)

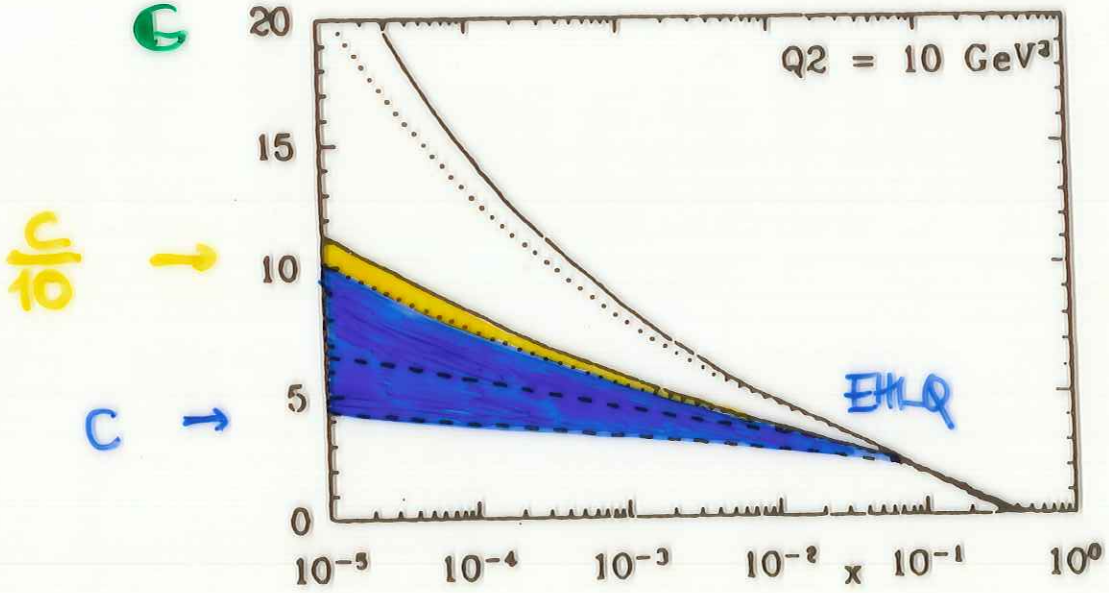

b

$C = C(\hat{Q}_0^2)$

$\hat{Q}_0 = \hat{Q}_0(R_{sc})$

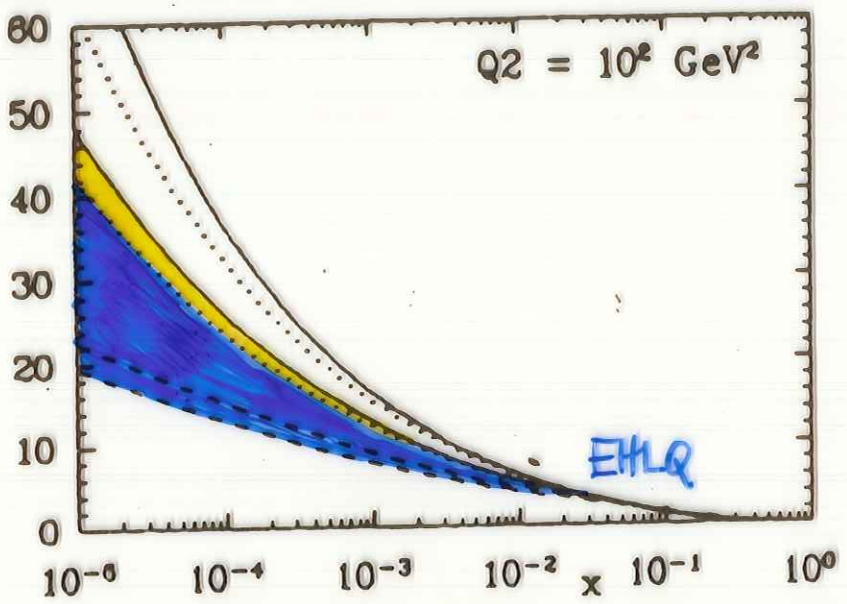

c

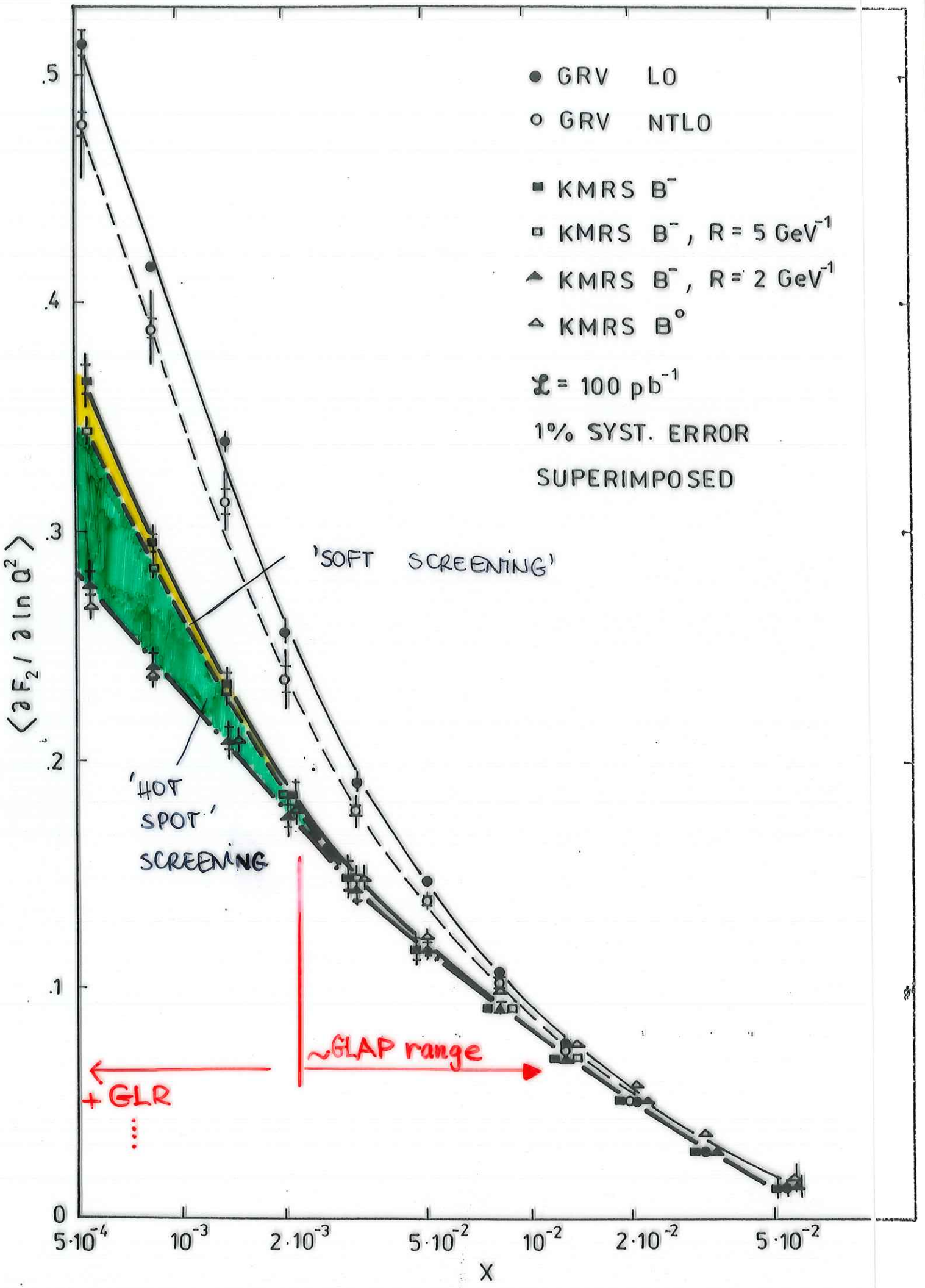
GRV LO
GRV NTLO
KMRS B⁻
KMRS B⁻, R = 5 GeV⁻¹
KMRS B⁻, R = 2 GeV⁻¹
KMRS B°
ℒ = 100 pb⁻¹
1% SYST. ERROR
SUPERIMPOSED
'SOFT SCREENING'
'HOT SPOT' SCREENING
~GLAP range
+ GLR
⟨∂F₂ / ∂ ln Q²⟩
X
.5
.4
.3
.2
.1
0
5·10⁻⁴
10⁻³
2·10⁻³
5·10⁻²
10⁻²
2·10⁻²
5·10⁻²

BARTELS, JB, SCHULER

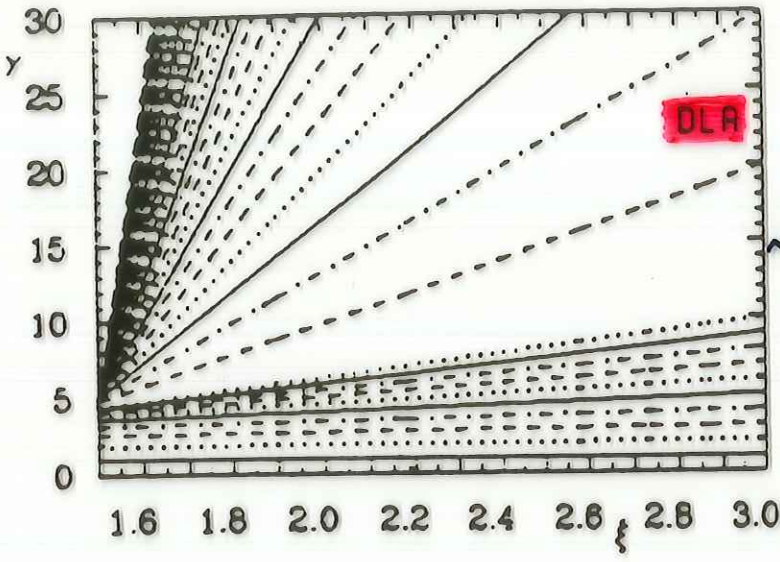

~AP

a

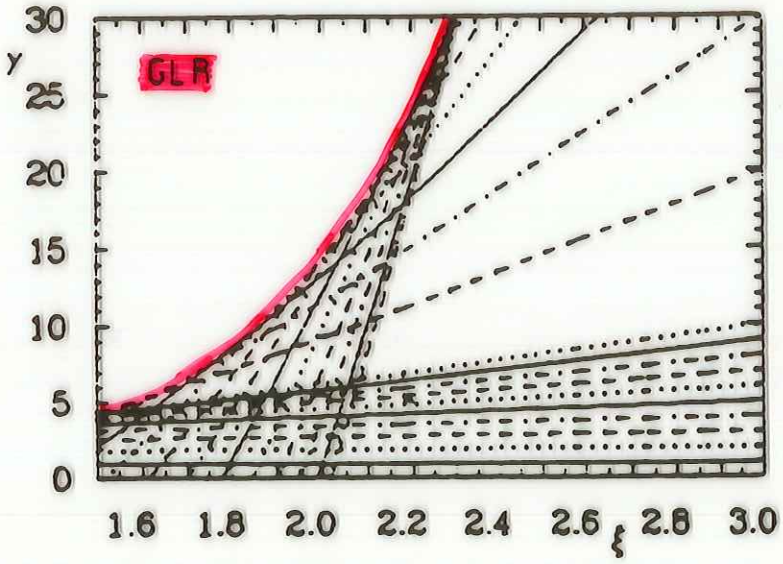

TRAJECTORIES STARTING BELOW

b

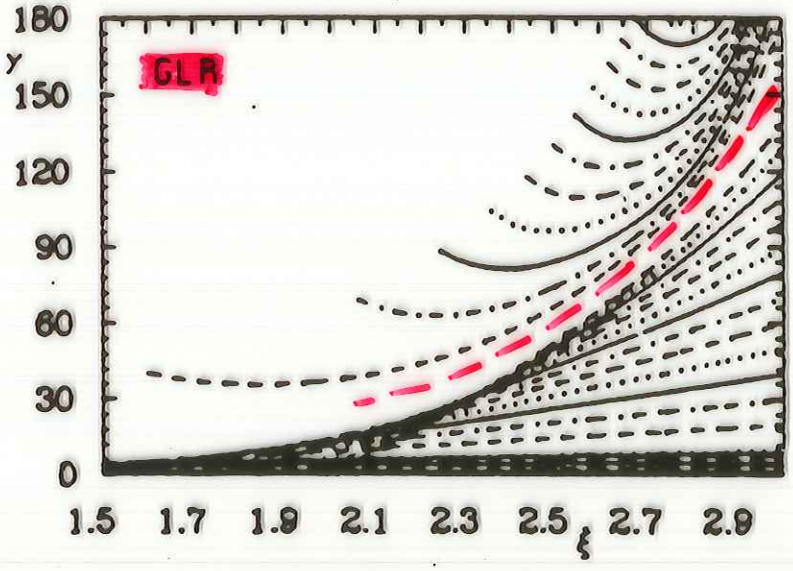

ABOVE THE 'CRITICAL' LINE

$F_L(x, Q^2)$

$$f_L^{qG}(K^2, x, Q^2) = -\frac{1}{4\pi}\int dPS^{(2)} x T_{\mu\nu}^2 \widehat{W}^{\mu\nu}$$
$$= \frac{\alpha_s e_q^2}{4\pi}\left\{\frac{4Q^4}{K^4 x}G_{1L}(\beta,\zeta) + \frac{xQ^2}{K^2}\frac{1}{\sqrt{1-\zeta}}\log\left|\frac{1+\sqrt{1-\zeta}}{1-\sqrt{1-\zeta}}\right| G_{2L}(\beta,\zeta) + \frac{2xQ^2}{K^2}G_{3L}(\beta,\zeta)\right\}$$

with

$$\zeta = \frac{4K^2x^2}{Q^2}$$

and

$$G_{iL}(\beta,\zeta) = -\sum_{j=0}^{4} g_{ji}^L(\beta)\left(\frac{\zeta}{W(\zeta)}\right)^j$$

where

$$W(\zeta) = 1 - \zeta + \sqrt{1-\zeta}$$

→ TAB.

$$f_L^{qG(0)}(x, Q^2) = \frac{8x^3}{Q^2}\frac{1}{4\pi}\int dPS^{(2,0)} P_\mu P_\nu \widehat{W}^{\mu\nu} = \frac{2}{\pi}e_q^2\alpha_s x^2(1-x)$$

$\lim_{k^2\to 0}$:

$$F_L(x,Q^2) = \int_x^1 \frac{d\eta}{\eta} f_L\left(\frac{x}{\eta}\right)\eta\, G(\eta, Q_0^2) + \int_x^1 \frac{d\eta}{\eta}\int_{Q_0}^{k^2_{max}} dk^2\, f_L\left(\frac{x}{\eta}, \frac{k^2}{Q^2}\right)\frac{\partial\eta\, G(\eta,k^2)}{\partial k^2}$$

$$
\begin{aligned}
g_{01}^{(L)}(\beta) &= -\frac{1}{8} + \frac{1}{4}\cos\beta - \frac{1}{4}\cos^3\beta + \frac{1}{8}\cos^4\beta \\
g_{02}^{(L)}(\beta) &= -\frac{1}{4} + 2\cos\beta - \cos^2\beta - 3\cos^3\beta + \frac{9}{4}\cos^4\beta \\
g_{03}^{(L)}(\beta) &= -\frac{1}{4} + 6\cos\beta - \frac{9}{2}\cos^2\beta - 10\cos^3\beta + \frac{35}{4}\cos^4\beta \\
g_{11}^{(L)}(\beta) &= \cos\beta - \frac{3}{4}\cos^2\beta - \frac{3}{2}\cos^3\beta + \frac{5}{4}\cos^4\beta \\
g_{12}^{(L)}(\beta) &= \frac{1}{4} + \frac{13}{2}\cos\beta - \frac{15}{2}\cos^2\beta - \frac{21}{2}\cos^3\beta + \frac{45}{4}\cos^4\beta \\
g_{13}^{(L)}(\beta) &= 1 + 18\cos\beta - 24\cos^2\beta - 30\cos^3\beta + 35\cos^4\beta \\
g_{21}^{(L)}(\beta) &= \frac{3}{16} + \frac{9}{8}\cos\beta - \frac{9}{4}\cos^2\beta - \frac{15}{8}\cos^3\beta + \frac{45}{16}\cos^4\beta \\
g_{22}^{(L)}(\beta) &= \frac{5}{4} + \frac{27}{4}\cos\beta - 15\cos^2\beta - \frac{45}{4}\cos^3\beta + \frac{75}{4}\cos^4\beta \\
g_{23}^{(L)}(\beta) &= \frac{7}{2} + 18\cos\beta - 42\cos^2\beta - 30\cos^3\beta + \frac{105}{2}\cos^4\beta \\
g_{31}^{(L)}(\beta) &= \frac{3}{16} + \frac{6}{16}\cos\beta - \frac{15}{8}\cos^2\beta - \frac{5}{2}\cos^3\beta + \frac{35}{4}\cos^4\beta \\
g_{32}^{(L)}(\beta) &= \frac{9}{8} + \frac{9}{4}\cos\beta - \frac{45}{4}\cos^2\beta - \frac{15}{4}\cos^3\beta + \frac{105}{8}\cos^4\beta \\
g_{33}^{(L)}(\beta) &= 3 + 6\cos\beta - 30\cos^2\beta - 10\cos^3\beta + 35\cos^4\beta \\
g_{41}^{(L)}(\beta) &= \frac{3}{64} - \frac{15}{32}\cos^2\beta + \frac{35}{64}\cos^4\beta \\
g_{42}^{(L)}(\beta) &= \frac{9}{32} - \frac{45}{16}\cos^2\beta + \frac{105}{32}\cos^4\beta \\
g_{43}^{(L)}(\beta) &= \frac{3}{4} - \frac{15}{2}\cos^2\beta + \frac{35}{4}\cos^4\beta
\end{aligned}
$$

$$ep \to \nu_e H^0 X + O(\alpha L) + O(\alpha_s)$$
$H^0 \hookrightarrow b\bar{b}$

JB, VAN OLDENBORGH, RÜCKL.

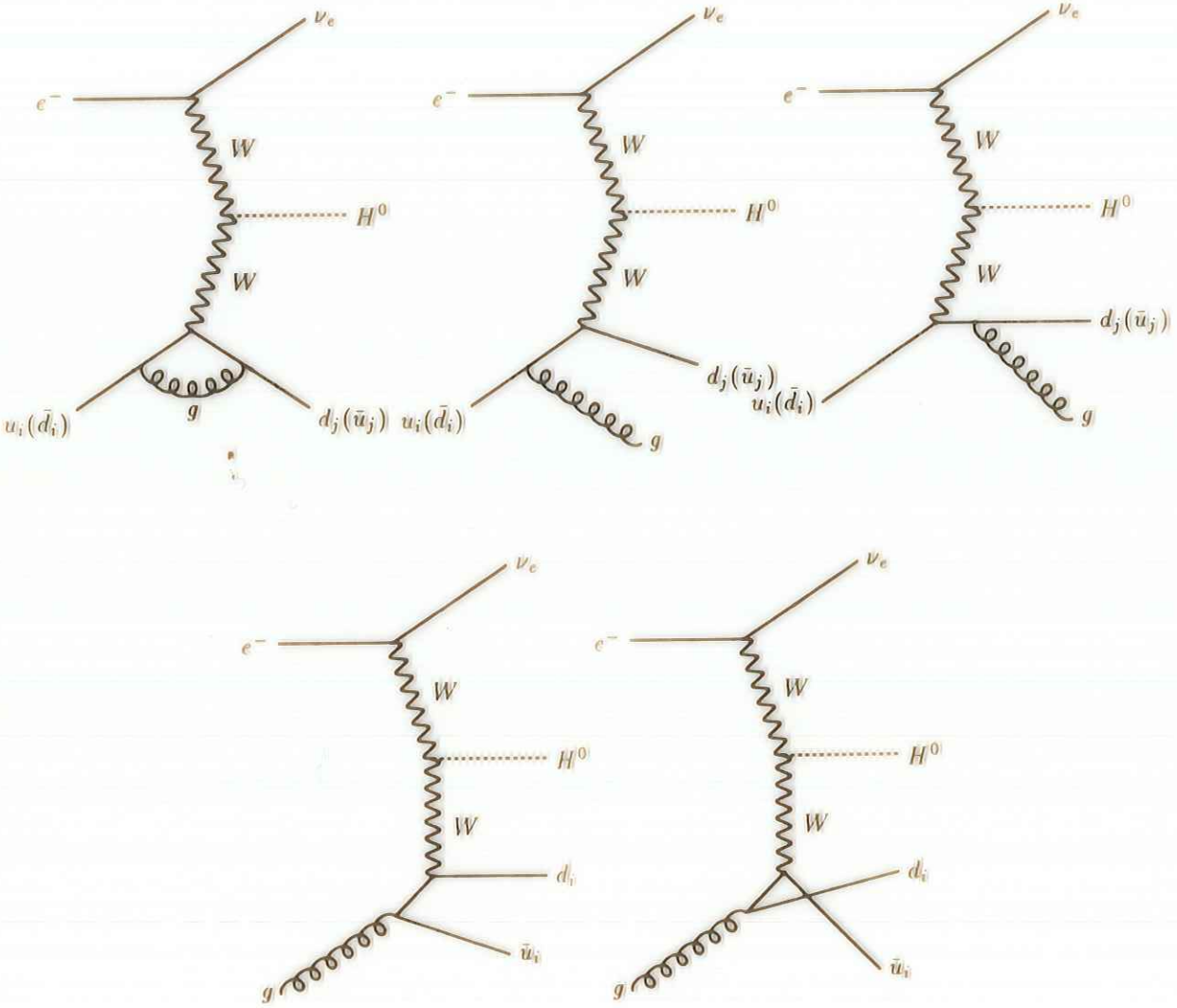

Figure 4: The $\mathcal{O}(\alpha_s)$ diagrams contributing to the QCD corrections at the hadronic vertex.

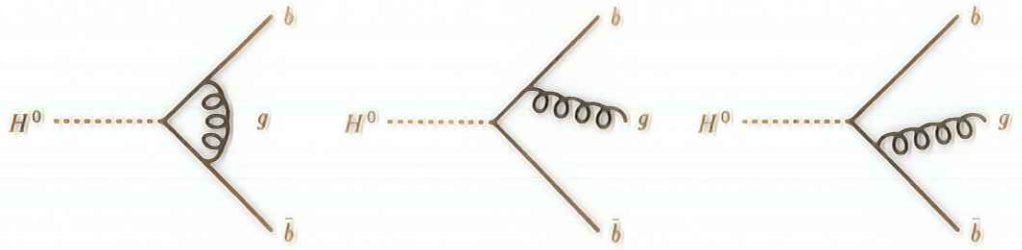

Figure 7: The $\mathcal{O}(\alpha_s)$ diagrams contributing to the QCD corrections to the decay vertex.

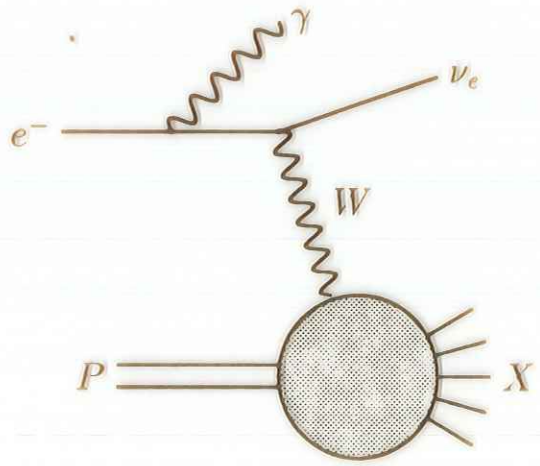

Figure 8: Diagram representing the leading QED correction to charged current ep processes.

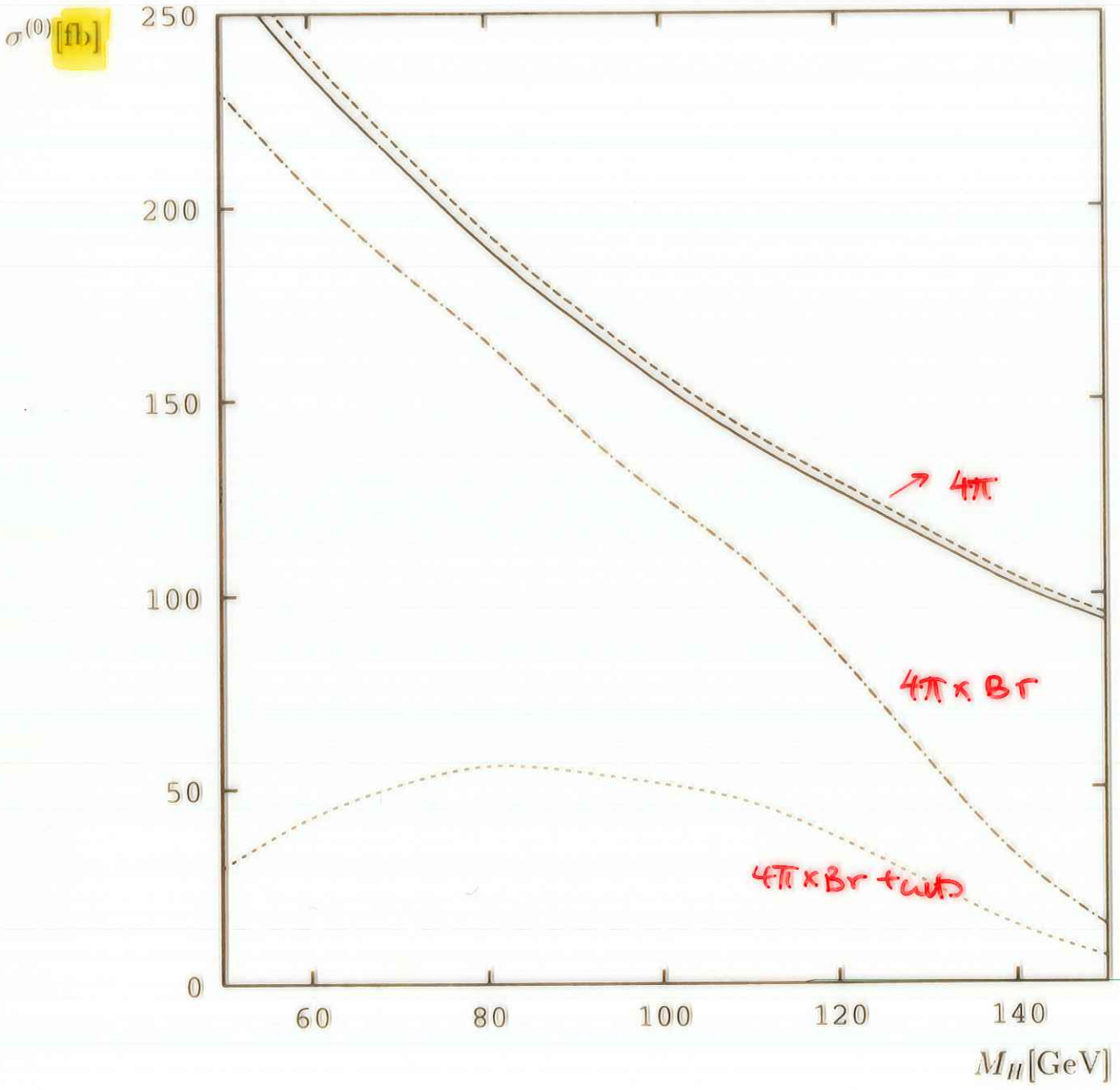

Figure 2: Born cross sections using the parton distributions by Morfin and Tung (MT2). Long-dashed line: $\sigma_{tot}^{(0)}$ for MT2($\overline{\rm MS}$); full line: $\sigma_{tot}^{(0)}$ for MT2(DIS); dash-dotted line: $\sigma_{tot}^{(0)} \times Br(H^0 \to b\bar{b})$ for MT2(DIS); short-dashed line: $\sigma_{obs}^{(0)}$ as defined in the text.

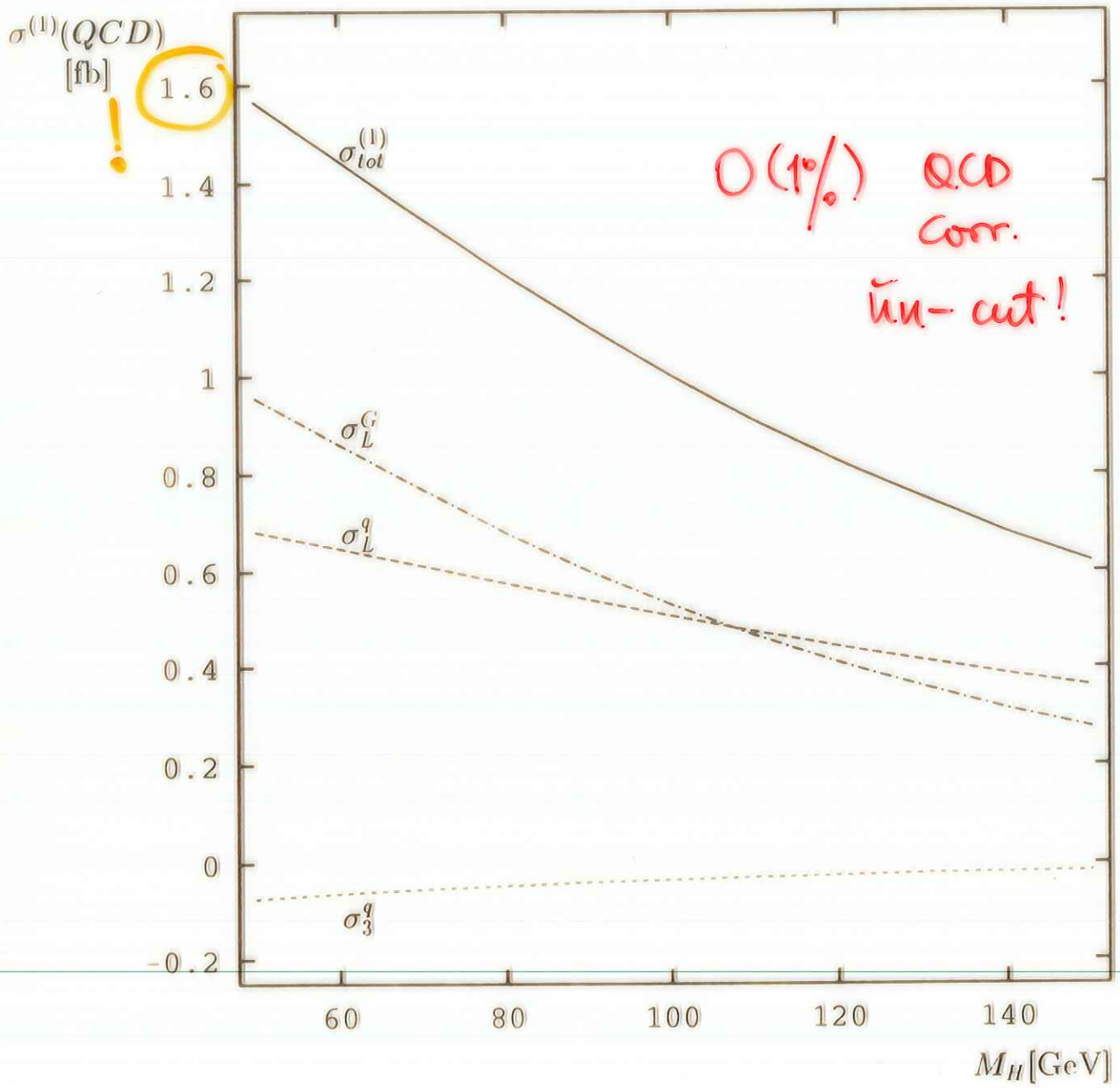

Figure 5: The $O(\alpha_s)$ QCD corrections to σ_{tot} in the DIS scheme. Full line: $\sigma^{(1)}_{tot}(QCD)$, long-dashed line: σ^{q}_{L}, dash-dotted line: σ^{G}_{L}, and short-dashed line: σ^{q}_{3}.

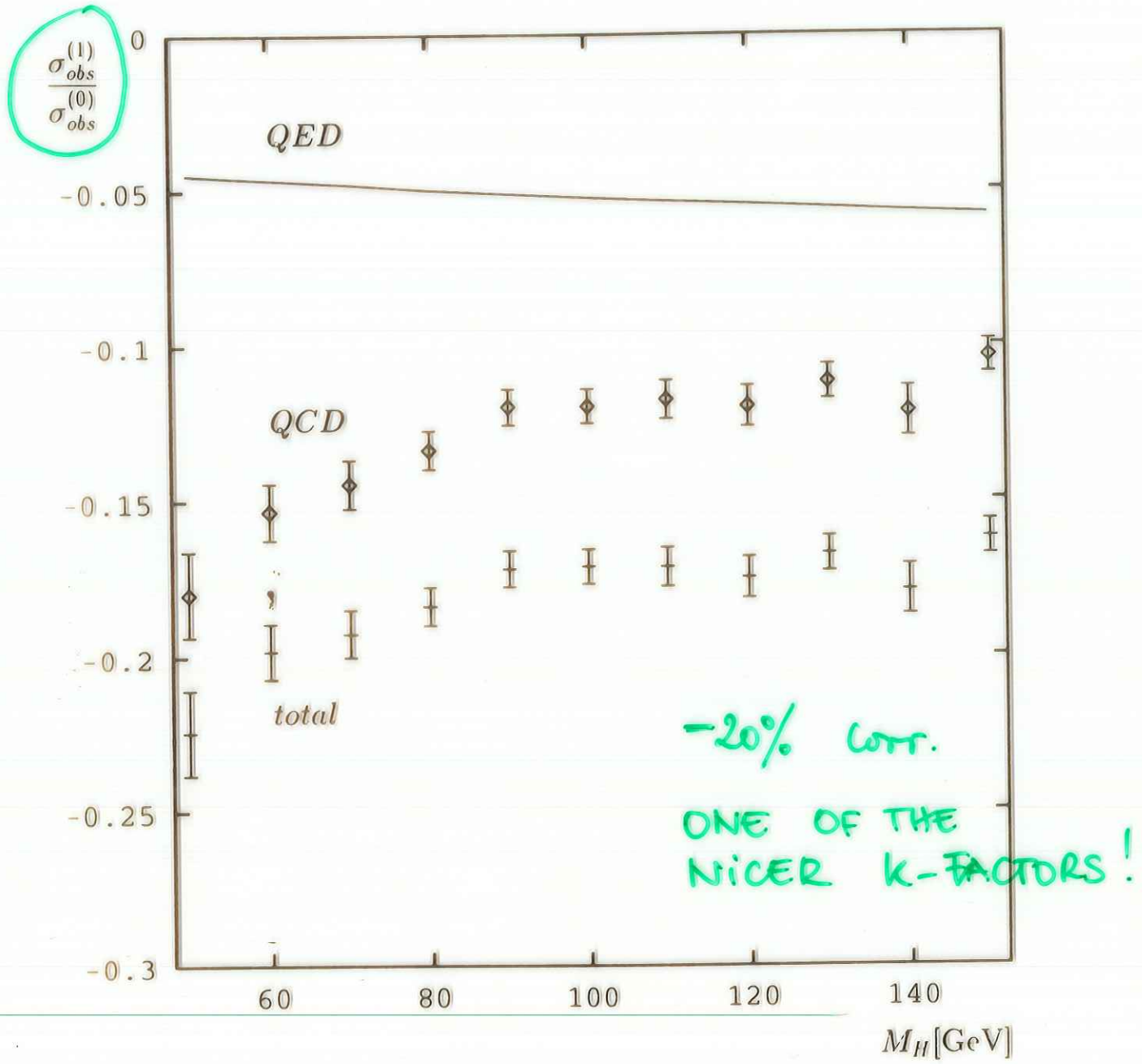

Figure 10: The relative corrections $\sigma^{(1)}_{obs}/\sigma^{(0)}_{obs}$ to the observable cross section for $e^- p \to \nu H^0 X\,; H^0 \to b\bar{b}$, including the cuts given in section 2. The QCD and the leading QED corrections are shown separately. The error bars indicate the statistical precision of the Monte Carlo calculation.